Research Square

Preprints are preliminary reports that have not undergone peer review.
They should not be considered conclusive, used to inform clinical practice,
or referenced by the media as validated information.

Integrating intraspecific genetic variation and species distribution models to predict the potential impacts of climate change on Sepia pharaonis

Haomiao Chi

c23014877440163.com

Ocean University of China

Xiaoyang Wang

Ocean University of China

jian Zheng

Ocean University of China

Xiaodong Zheng

Ocean University of China

Research Article

Keywords:

Posted Date: November 9th, 2026

DOI: https://doi.org/10.21203/rs.3.rs-11650723/v1

License: This work is licensed under a Creative Commons Attribution 4.0 International License.
Read Full License

Additional Declarations: No competing interests reported.

Integrating intraspecific genetic variation and species distribution models to predict the potential impacts of climate change on *Sepia pharaonis*

Haomiao Chi[a, b] Xiaoyang Wang[a, b] Jian Zheng[a, b] Xiaodong Zheng[a, b, *]

[a] Key Laboratory of Mariculture, Ministry of Education, Ocean University of China, Qingdao 266003, China

[b] Key Institute of Evolution & Marine Biodiversity (IEMB), Ocean University of China, Qingdao 266003, China

Abstract

Incorporating intraspecific genetic variation into species distribution models (SDMs) can improve the accuracy of species distribution predictions. However, few studies have evaluated its importance for SDMs. The pharaoh cuttlefish (*Sepia pharaonis*), widely distributed across the Indo-Pacific, exhibits genetic differentiation. In this study, we investigated intraspecific genetic variation based on mitochondrial *COI* and *16S* rRNA sequences and integrated genetic information into SDMs to predict distribution shifts and ecological vulnerability at the lineage level. Phylogeographic analysis identified five lineages: Red Sea (RE), Australian (AU), Persian Gulf and Oman Sea (PE), central Indian Ocean (CE), and western Pacific (WE) lineages. These lineages exhibited substantial niche differentiation. At the species level, *S. pharaonis* preferred waters with high primary productivity. Suitable habitats were projected to expand southward, and relatively high ecological vulnerability was predicted in the Persian Gulf, the South China Sea, and Malaysian coastal waters. Lineage-level models revealed divergent climate responses masked by the species-level model. The CE and PE lineages preferred high productivity environments, consistent with the species-level SDM prediction, whereas the AU and WE lineages exhibited stronger tolerance to low-productivity environments. The WE and CE lineages faced higher risks of range contraction under SSP5-8.5. The WE lineage also harbored lower genetic diversity, potentially increasing its vulnerability to climate change. In contrast, the AU and PE lineages were projected to expand their suitable habitats eastward under most climate scenarios, reflecting their greater climate tolerances. This study provides crucial information for climate-adaptive conservation and management based on more precise taxonomic units for *S. pharaonis*.

Keywords: *Sepia pharaonis*, climate change, species distribution models, intraspecific genetic variation, habitat suitability

[*] Corresponding author at: Key Laboratory of Mariculture, Ministry of Education, Ocean University of China, Qingdao 266003, China.
E-mail address: xdzheng@ouc.edu.cn (X. Zheng).

1. Introduction

Climate change driven by anthropogenic greenhouse gas emissions has significantly altered the marine environment, including surface water temperature, salinity, sea-ice extent, currents, and pH (Fox-Kemper et al. 2021). These changes are expected to have major effects on marine life at both the ecological and physiological levels (Sampaio et al. 2021; Fernandes Guerreiro et al. 2023b; Zheng et al. 2023; Zheng et al. 2024). Cephalopods exhibit rapid growth, short lifespans, and limited generation overlap, making them highly sensitive to climate change (Xiang et al. 2025). They are keystone species in marine ecosystems and play a crucial role in maintaining biodiversity and ecological balance (Vinagre et al. 2025). Given their high sensitivity to climate change and important ecological and economic roles, several studies have indicated that cephalopods may shift their distributions toward higher latitudes or deeper waters to search for suitable niches under climate change (Schickele et al. 2021; Fernandes Guerreiro et al. 2023a; Fernandes Guerreiro et al. 2023b; Wang et al. 2026). Thus, exploring the potential distribution of economically and ecologically important cephalopod species under future climate scenarios can provide valuable information for the effective conservation and management of these species (Huang et al. 2024).

The pharaoh cuttlefish, *Sepia pharaonis* Ehrenberg, 1831, is an important neritic cephalopod that supports fisheries and aquaculture throughout the Indo-Pacific (Song et al. 2021). Its short lifespan and sensitivity to climate change can produce rapid changes in abundance and distribution, complicating stock assessments and fisheries management (Pecl and Jackson 2008; Arkhipkin et al. 2021). For example, Sasikumar et al. (2013) reported that rising temperatures accelerated growth and advanced sexual maturation in the early post-monsoon recruits of *S. pharaonis*. Between 1997 and 2019, the catching of *S. pharaonis* in the waters of southern Iran declined by approximately 44%, from about 9,000 to 5,000 t. This sharp decline may have been associated with excessive fishing pressure, as annual catches exceeded the estimated maximum sustainable yield (Hashemi and Doustdar 2021). Meanwhile, the IUCN Red List assessment classifies *S. pharaonis* as Data Deficient (DD), indicating that insufficient information is available to assess its risk of extinction (Barratt and Allcock 2012). Existing research on *S. pharaonis* has focused on phylogeography, reproductive biology, aquaculture, and fishery exploitation, yet relatively few studies have investigated how climate change affects its habitat suitability. Therefore, it is essential to predict its suitable habitat and distribution shifts under current and future climate scenarios. Moreover, different lineages within the same species may exhibit distinct responses to climate change. Previous studies have provided preliminary evidence of genetic differentiation in *S. pharaonis* (Farhadi and Anderson 2021). This genetic differentiation may be associated with differences in environmental tolerance and ecological preferences among lineages. Thus, it is critical to characterize the ecological niches and geographic distribution patterns of its distinct lineages to improve predictions of their

responses to climate change.

Species distribution models (SDMs) represent very useful tools and have been widely applied in habitat suitability modeling over the past few decades (Elith and Leathwick 2009; Zurell et al. 2020; Davies et al. 2023). These models establish relationships between species distributions and environmental conditions based on species occurrence data and environmental variables. They can be used to predict the future potential distribution of species when predictor variables are derived from future climate scenarios (Sillero et al. 2021). Traditional SDMs commonly assume ecological niche conservatism, meaning that species' environmental tolerances remain constant over time. This assumption ignores potential local adaptation associated with population divergence, which may compromise the accuracy of model predictions (Hällfors et al. 2016; Ikeda et al. 2017; Lu et al. 2024). For species with substantial genetic differentiation, overlooking ecological differences among geographic lineages may obscure their distinct responses to environmental change (D'Amen et al. 2013; Hällfors et al. 2016; Shan et al. 2025). Meanwhile, several studies have emphasized that considering genetic structure and local adaptation when constructing SDMs can improve model performance (Gonzalez et al. 2011; Ikeda et al. 2017; Chardon et al. 2020). For example, Wu et al. (2024) demonstrated that integrating genetic structure into modeling enables lineage-level SDMs to provide a more detailed understanding of changes in population distributions. Therefore, constructing lineage-level SDMs can improve predictions of potential distributions and facilitate a more mechanistic understanding of species' adaptations and responses to changing environmental conditions.

In this study, we characterized the genetic structure and ecological niche differentiation of *S. pharaonis* and projected its distribution shifts under different climate scenarios at both the species and lineage levels. The main objectives of this research were to (1) integrate global genetic data to assess the genetic diversity and differentiation of *S. pharaonis*; (2) quantify niche differentiation among lineages and construct SDMs at the species and lineage levels to predict current suitable habitat; (3) predict changes in suitable habitat area, habitat gains and losses, and distribution centroid shifts under future climate scenarios. Our findings can provide a scientific basis for developing adaptive conservation and management strategies for *S. pharaonis*.

2. Materials and methods

2.1 Data collection and processing

This study compiled a total of 91 *COI* sequences and 51 *16S* rRNA sequences from five geographic regions: the Red Sea, Australia, the Persian Gulf and the Oman Sea, the central Indian Ocean, and the western Pacific. The *COI* dataset included 15, 6, 14, 40, and 16 sequences

from these regions, respectively, and the *16S* rRNA dataset included 5, 5, 12, 13, and 16 sequences, respectively. Compared with the datasets used in previous studies, we added 44 *COI* sequences and 20 *16S* rRNA sequences from GenBank (http://www.ncbi.nlm.nih.gov/) and published literature. The associated source publications are listed in Table S1. First, the *COI* and *16S* rRNA sequences were aligned using MAFFT (Katoh et al. 2002). The local ambiguities in the alignments were removed with Gblocks under default parameters, and the resulting fragments were concatenated (Castresana 2000). Subsequently, measures of population genetic diversity (i.e., haplotype diversity, nucleotide diversity, and the average number of nucleotide differences) were calculated with DnaSP6 (Rozas et al. 2017). Next, analysis of molecular variance (AMOVA) was performed in Arlequin v3.5.2.2, with significance tested through 10,000 permutations (Excoffier and Lischer 2010). Genetic differentiation among populations was assessed by F_{st} values using Arlequin v3.5.2.2. In addition, haplotypes were identified from aligned sequences, and a median-joining haplotype network was constructed using PopART v1.7 (Leigh and Bryant 2015). Finally, a phylogenetic tree was constructed using the maximum likelihood (ML) method based on the Kimura 2-parameter (K2P) model in MEGA 12 (Kumar et al. 2024) and visualized using iTOL v6 (Letunic and Bork 2024).

A large number of species occurrence records enable more comprehensive characterization and modeling of the species' ecological niche (Breiner et al. 2015). Our study collected reliable occurrence data from the Global Biodiversity Information Facility (GBIF, https://www.gbif.org) and the Ocean Biogeographic Information System (OBIS, https://obis.org). In addition, we performed an exhaustive literature search spanning the period 2000–2025 to expand spatial sampling coverage and improve the predictive reliability of species distribution models. From the initial search yield of more than 4,590 articles, we retained only 35 articles that reported specific location data or sampling maps (Table S2). Subsequently, species occurrence data were extracted from these sampling maps using the georeferencing module in ArcGIS 10.8.1. Next, the R package *spThin* was used to spatially thin the occurrence records, retaining only one record per 5.5 km × 5.5 km grid cell to minimize spatial autocorrelation (Wang et al. 2026). Finally, a total of 1,177 occurrence records were retained, including 8, 873, 25, 175, and 96 for the RE, AU, PE, CE, and WE lineages of *S. pharaonis*, respectively. Because RE contained only 8 occurrence records after spatial filtering, it was not included in the lineage-level SDM projections to avoid unreliable model fitting and overinterpretation (Li et al. 2022). Therefore, lineage-level SDMs were constructed only for the AU, PE, CE, and WE lineages (Fig. 1).

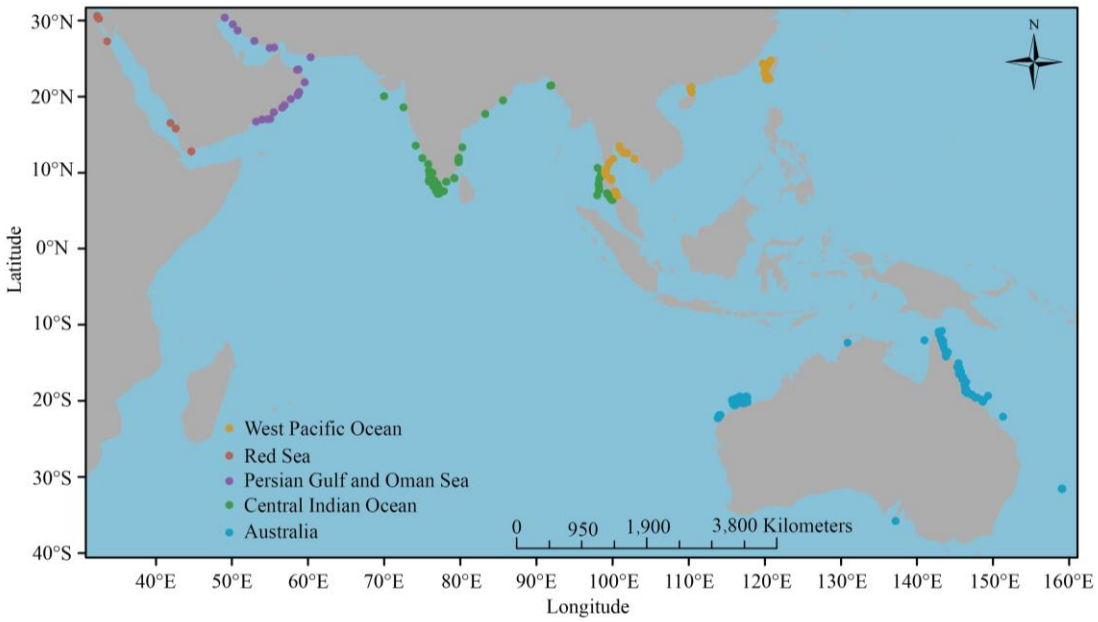


Fig. 1 Distribution of available occurrence points for *Sepia pharaonis*.

2.2 Environmental variables

Given data availability and the potential relationships between species occurrence and environmental variables, we initially selected seven environmental variables that may impact the distribution of *S. pharaonis*: temperature, salinity, topographic slope, depth, primary productivity, dissolved oxygen, and pH. Temperature was included because experiments have shown that it affects cuttlefish egg hatching (Palmegiano and D'Apote 1983). Salinity was included because experimental studies have shown that it affects embryonic development and physiological responses to low salinity in this species (Peng et al. 2017; Wu et al. 2021). Depth and topographic slope were included to represent bathymetric variation across the study area. Given the lack of spatially comprehensive prey-distribution data, we used primary productivity as a proxy for food-web productivity (Shan et al. 2025). Dissolved oxygen and pH were considered because oxygen availability can limit cuttlefish distributions and lower pH can alter cuttlebone calcification (Fernandes Guerreiro et al. 2023a).

With a spatial resolution of 0.05º (approximately 5.5 km × 5.5 km at the equator), all environmental data were obtained from Bio-ORACLE version 3 (Tyberghein et al. 2012; Assis et al. 2024). Considering that *S. pharaonis* is a demersal species, environmental layers were derived from bottom-water conditions (Assis et al. 2024). The average values of environmental variables from 2000 to 2020 were taken to represent the current environmental conditions. Pearson correlation coefficients were calculated for each pair of variables to minimize potential

bias caused by high covariance between variables (Johnston et al. 2018). If the absolute value of the correlation coefficient between two variables exceeded 0.8, the less important variable was excluded (McMahan et al. 2020). For the WE lineage, mean water temperature (Tm) and primary productivity (Pri) showed a relatively high Pearson correlation coefficient (r = 0.85). Although this correlation exceeded the 0.8 threshold, both variables were retained because temperature and primary productivity are considered ecologically important factors influencing the distribution and population dynamics of *S. pharaonis* (Palmegiano and D'Apote 1983; Ottmann et al. 2024). Ultimately, Tm (mean water temperature), Sal (mean salinity), and Pri (mean primary productivity) were the three environmental variables kept for subsequent analysis (Figs. S1–S5).

For future climate scenarios, Bio-ORACLE provides standardized climate layers based on climate projections from the Coupled Model Intercomparison Project Phase 6 (CMIP6). These projections use the Shared Socioeconomic Pathway (SSP) scenarios, which combine socioeconomic development pathways with different levels of greenhouse gas emissions (Burgess et al. 2023). We considered three future climate scenarios from CMIP6: SSP1-2.6, corresponding to a sustainability oriented low emission pathway; SSP2-4.5, representing an intermediate emission pathway; and SSP5-8.5, representing a high emission, fossil fuel dominated pathway. Under the three SSP scenarios, projections were conducted for two future periods: 2051–2060 and 2091–2100 (Mahmud and Osawa 2026; Wang et al. 2026).

2.3 Niche differentiation assessment

Three environmental predictors were used to describe the environmental conditions where *S. pharaonis* occurred. We performed principal component analysis (PCA) on the three environmental predictor variables (Tm, Sal, and Pri) to transform them into orthogonal principal components (Fig. S6). We then used the R package *hypervolume* (Blonder et al. 2025) to compute three-dimensional hypervolumes for each lineage (AU, CE, PE, and WE). The hypervolume represents the size of the niche space occupied by each lineage. Subsequently, the R package *BAT* was used to conduct overlap analysis of hypervolumes among lineages to assess niche differentiation (Cardoso et al. 2026). The total niche differentiation (β_{Total}) consists of two components: niche shift, which represents the replacement of space between the hypervolumes occupied by the lineages, and niche contraction or expansion, which refers to the net differences in the spatial extent encompassed by each niche hypervolume (Carvalho and Cardoso 2020; Mammola and Cardoso 2020). β_{Total} ranges from 0 to 1, with higher values indicating larger dissimilarity between two hypervolumes (Carvalho and Cardoso 2020; Mammola and Cardoso 2020).

2.4 Modeling procedures

We used 10 modeling techniques based on the *biomod2* package in the R platform

(Thuiller et al. 2024). In the study area, given the practical difficulty of obtaining true absence data, we generated pseudo-absence points for each modeling unit equal to ten times the number of occurrence records (Barbet-Massin et al. 2012). The limited number of occurrence records available for the lineages of *S. pharaonis* may lead to model overfitting. To overcome this limitation, we applied the ensemble of small models (ESMs) strategy using the R package *ecospat*, which is specifically designed for species with limited occurrence records (Breiner et al. 2015; Di Cola et al. 2017; Wu et al. 2024). We evaluated model performance using the area under the receiver operating characteristic curve (AUC) and the true skill statistic (TSS). Only models that met performance thresholds (TSS > 0.8 and AUC > 0.9) were retained and incorporated into an ensemble forecast through a weighted averaging approach (Marmion et al. 2009). In addition to TSS and AUC, we used the continuous Boyce index (CBI), a threshold-independent metric, to measure the difference between ESM predictions and a random distribution of known species presence points across the prediction gradient (Manzoor et al. 2018).

We then used a permutation approach to calculate the relative importance of each predictor variable and generated response curves for the three environmental factors (Huang et al. 2024). Species distribution projections for the present (2000–2020) and future periods (2051–2060 and 2091–2100) under three SSP scenarios were performed using the ensemble model with the BIOMOD_Projection function in the *biomod2* package. Habitat suitability was expressed as a probability ranging from 0 to 1. For each scenario, we also quantified habitat range shifts and distribution centroid movements. Ecological vulnerability (VE) was quantified as the signed difference between future and present suitability. Positive values indicate habitat gain or increased suitability, whereas negative values indicate habitat loss or decreased suitability (Turan and Soldo 2026).

3. Results

3.1 Population genetic analysis

The genetic diversity analysis results of *COI* and *16S* rRNA sequences for *S. pharaonis* across five populations are summarized in Table 1. For the *COI* sequences, the total number of segregating sites across all populations was 86, the overall haplotype diversity was 0.958, the nucleotide diversity was 0.0489, and the average number of nucleotide differences was 21.041. Among the five populations, the WE population exhibited the lowest haplotype and nucleotide diversity, while the RE population displayed the highest genetic diversity. For the *16S* rRNA sequences, the total number of segregating sites was 37, the overall haplotype diversity was 0.902, the nucleotide diversity was 0.0253, and the average number of nucleotide differences was 10.631. The PE population exhibited the lowest haplotype and nucleotide diversity among the five populations based on the *16S* rRNA data. Both *COI* and *16S* rRNA sequences showed

high nucleotide diversity (> 0.005) and haplotype diversity (> 0.5), indicating high genetic diversity within *S. pharaonis*.

Table 1. Genetic diversity parameters of five populations in *Sepia pharaonis* based on *COI* and *16S* rRNA sequences.

Gene	Populations	*S*	H	*H*d	π	*K*
COI	AU	3	4	0.867	0.0028	1.200
	CE	18	17	0.886	0.0052	2.281
	PE	12	9	0.923	0.0056	2.451
	RE	27	8	0.924	0.0244	10.476
	WE	4	4	0.442	0.0016	0.700
16S rRNA	AU	2	3	0.700	0.0019	0.800
	CE	4	5	0.756	0.0029	1.205
	PE	0	1	0.000	0.0000	0.000
	RE	1	2	0.400	0.0010	0.400
	WE	5	5	0.742	0.0027	1.133

Genetic diversity parameters included the number of segregating sites (*S*), the number of haplotypes (H), haplotype diversity (*H*d), nucleotide diversity (π), and average number of nucleotide differences (*K*).

The population structure among five populations of *S. pharaonis* was assessed using analysis of molecular variance (AMOVA) and pairwise F_{st} values. AMOVA results based on the *COI* sequences showed that 88.06% ($P < 0.001$) of genetic variation occurred among populations, while 11.94% occurred within populations. AMOVA results based on *16S* rRNA revealed that most genetic variation also occurred among populations, accounting for 94.14% ($P < 0.001$), with 5.86% occurring within populations (Table S3). These findings consistently indicated that most genetic variation in *S. pharaonis* was distributed among populations, with limited variation occurring within populations. Based on analyses of *COI* and *16S* rRNA sequences, pairwise F_{st} values among the five populations ranged from 0.7767 to 0.9784 (*COI*) and from 0.8796 to 0.9941 (*16S* rRNA). The results revealed highly significant genetic differentiation among the five populations ($P < 0.001$) (Fig. 2).

Haplotype networks based on mitochondrial *COI* and *16S* rRNA sequences were constructed for the AU, CE, PE, RE, and WE populations. As shown in Fig. S7, the *COI*

network contained 42 haplotypes and showed clear clustering by population. Haplotypes were clearly differentiated among populations, with the major groups separated by multiple mutational steps and connected through inferred intermediate haplotypes. The *16S* rRNA network contained 16 haplotypes and displayed a simpler topology, but the haplotypes were also largely grouped by population. No haplotype shared by all populations was observed in either network, further supporting the genetic differentiation among populations.

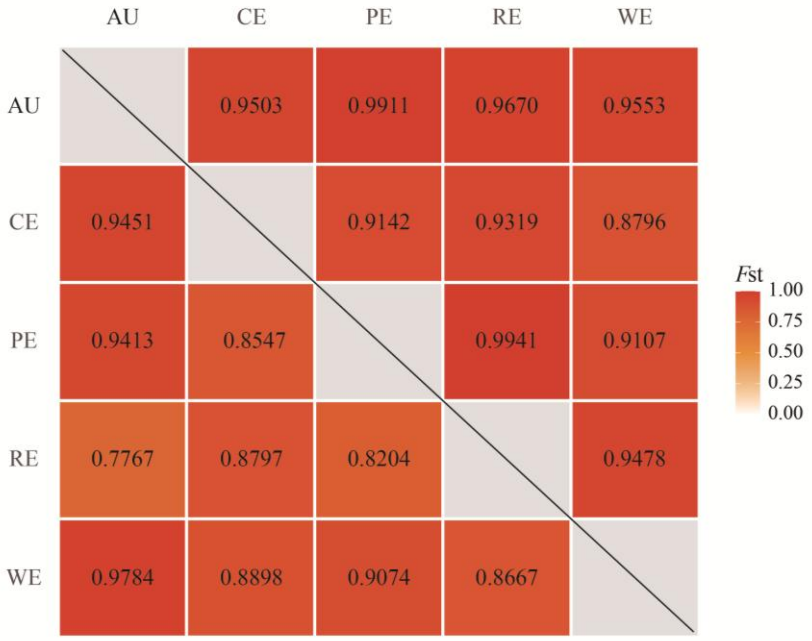


Fig. 2 F_{st} values among five populations of *Sepia pharaonis* based on *COI* (lower diagonal) and *16S* rRNA (upper diagonal) sequences.

Phylogenetic analyses based on *COI* and *16S* rRNA sequences showed clear genetic structuring within *S. pharaonis*. The major genetic lineages largely corresponded to the five geographically distinct areas: the AU lineage (Australia), the CE lineage (central Indian Ocean), the PE lineage (Persian Gulf and Oman Sea), the RE lineage (Red Sea), and the WE lineage (western Pacific). Overall, the phylogenetic patterns were consistent with the genetic differentiation revealed by AMOVA and pairwise F_{st} analyses (Table S3, Fig. 3).

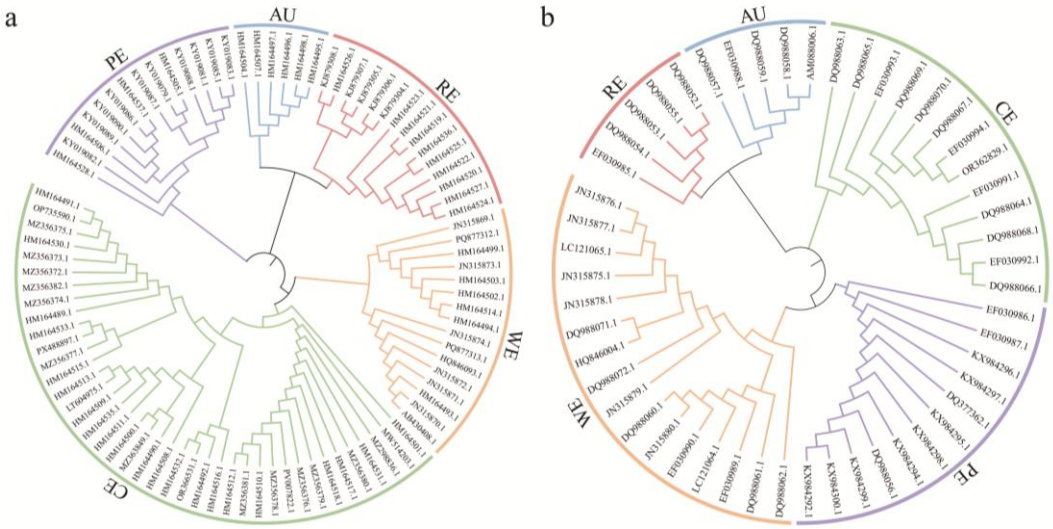


Fig. 3 Maximum likelihood (ML) phylogenetic tree based on *COI* (a) and *16S* rRNA (b) sequences, showing genetic structure among five populations in *Sepia pharaonis*. Bootstrap values above 70% are shown at the corresponding branches. Different colors represent different populations: blue represents the Australian lineage (AU), green represents the central Indian Ocean lineage (CE), purple represents the Persian Gulf and Oman Sea lineage (PE), red represents the Red Sea lineage (RE), orange represents the western Pacific lineage (WE).

3.2 Niche differentiation among four lineages

PC1 was mainly associated with Pri (40.6%) and Tm (37.4%), PC2 was dominated by Sal (76.4%), and PC3 was mainly explained by Pri (53.8%) and Tm (44.7%) (Fig. 4a). The three-dimensional hypervolumes for AU, CE, PE, and WE were 5.25, 291.77, 670.43, and 239.94, respectively. Comparison of β_{Total} values from hypervolume analyses revealed substantial niche differentiation among the four lineages. The AU lineage had a much narrower realized niche than the other lineages, and the high β_{Total} values primarily reflected differences in niche breadth rather than shifts in niche position. Niche differentiation between the PE and CE lineages was primarily driven by niche contraction/expansion, which accounted for 72.5% of β_{Total}. A similar pattern was observed between the PE and WE lineages, where niche contraction/expansion accounted for 67.5% of β_{Total}. In contrast, the niche differentiation between the CE and WE lineages was mainly due to niche shift, which contributed 62.5% of β_{Total}. The high β_{Total} values between the AU lineage and the other three lineages were almost entirely attributable to niche contraction/expansion, while niche shift contributed only 0%–0.1% (Table S4). The overall niche comparison among the four lineages indicated that their niche differentiation was mainly associated with PC2, which was mainly explained by Sal (Fig. 4b). Pairwise niche comparisons showed that niche differentiation between any two of the four lineages was also mainly

associated with PC2 (Figs. S8–S13).

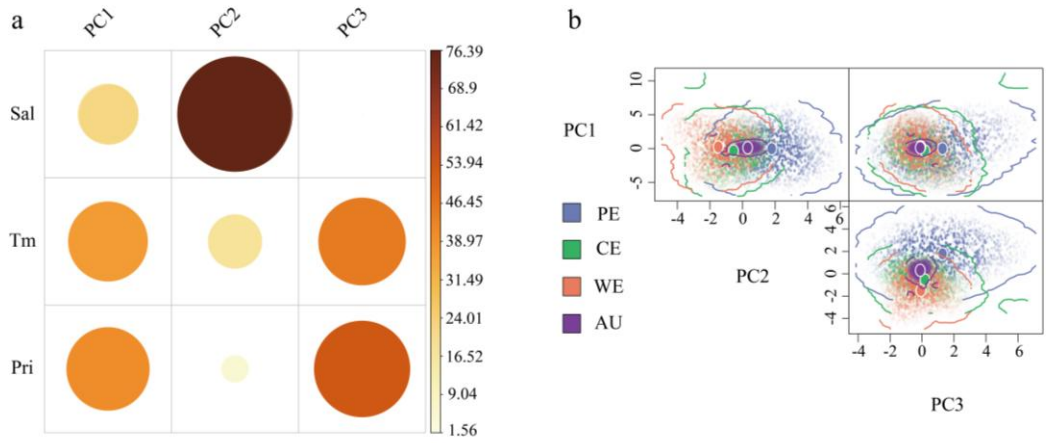


Fig. 4 Contributions of three environmental variables (Sal, Tm, Pri) to the three principal components (a); the realized niches of the four lineages of *Sepia pharaonis* quantified using three-dimensional hypervolumes (b). The large blue, green, orange, and purple points indicate the mean niche position of PE, CE, WE, and AU, respectively.

3.3 Model performance, variable importance and response curves

The predictive performance varied among modeling algorithms, as indicated by their different TSS and AUC values. ANN, CTA, FDA, GAM, GBM, GLM, Maxent, and RF all performed well (TSS > 0.8, AUC > 0.9) and were used to construct SDMs at both the species and lineage levels. However, MARS was excluded from the WE model due to poor performance (Tables S5–S7). The high TSS and AUC values of the models indicated high predictive accuracy. The models showed differences in the relative importance of the three environmental variables. The species-level model indicated that mean temperature was the most important predictor of the distribution of *S. pharaonis*, followed by primary productivity and salinity. The lineage-level models showed that salinity contributed most to the distribution of the AU and WE lineages, whereas temperature was the most important predictor of the distribution of the CE and PE lineages (Fig. S14). We also generated response curves for the three environmental variables (mean temperature, primary productivity, and salinity) at the species and lineage levels (Figs. S15–S19). At the species level, *S. pharaonis* showed low suitability at temperatures below 20 °C and preferred environments with high primary productivity. The species exhibited a relatively narrow salinity suitability range, with the highest suitability centered around a salinity of approximately 35. At the lineage level, the temperature suitability patterns of the four lineages were consistent with those at the species level. The AU, CE, and WE lineages preferred waters with salinity around 35, consistent with the species-level results, whereas the PE lineage showed a preference for salinity near 37. The CE and PE lineages

exhibited preferences consistent with the species-level pattern, with both favoring waters with high primary productivity. In contrast, the AU and WE lineages exhibited greater tolerance to environments with low primary productivity.

3.4 SDM projections

Predicted suitable habitats of *S. pharaonis* differed substantially between the species-level and lineage-level models under current climate conditions (Fig. 5). The highly suitable habitats predicted by the species-level SDM were primarily distributed in the South China Sea, the Gulf of Thailand, waters surrounding the Malay Archipelago, and northern Australian coastal waters. The model predictions were generally consistent with the known distribution of *S. pharaonis*. In contrast, the suitable habitat distributions predicted by the lineage-level models were markedly different from those predicted by the species-level model. The predicted suitable habitat areas for the PE and CE models were larger than those predicted by the species-level model. Compared with the species-level model, the PE model predicted more suitable habitat along the Persian Gulf, and the CE model predicted more suitable habitat along the coast of the northern Bay of Bengal and the eastern Andaman Sea. In contrast to these two lineages, the suitable habitat distribution predicted by the AU model was narrower than that predicted by the species-level model. The suitable habitat distributions predicted by the species-level model and the WE model were largely similar.

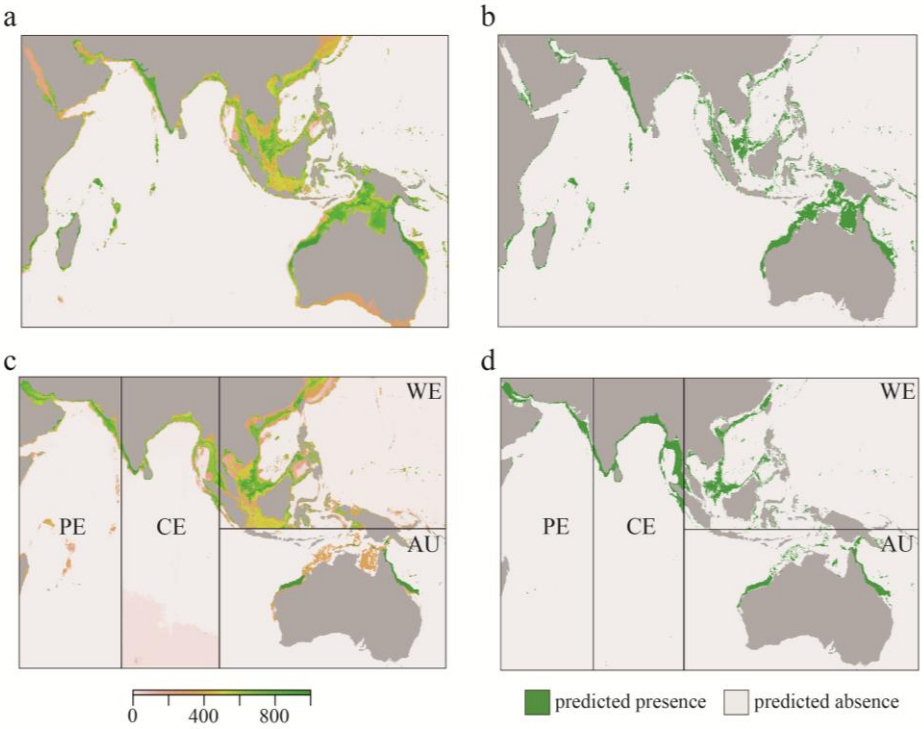


Fig. 5 Potential distribution projections based on models constructed at the species (a, b) and lineage (c, d) levels under current environmental conditions. A and c were continuous maps; b and d were binary maps.

Compared with current climate conditions, the suitable habitat of *S. pharaonis* in the species-level model showed varying degrees of southward expansion under all future climate scenarios, resulting in an overall trend of expansion (Fig. 7). The extent of expansion differed across climate scenarios and time periods. The areas of expansion were primarily distributed around the South China Sea, the Philippine Islands, the Indonesian Archipelago, northern Australia, and parts of the northwestern Indian Ocean (Fig. 6). Lineage-level predictions differed from those of the species-level model. The suitable habitat for the CE lineage showed limited but consistent contraction across all climate scenarios, with losses ranging from 16,274.50 to 28,435.00 km² and primarily confined to the eastern Bay of Bengal and the Andaman Sea. Under SSP5-8.5, the suitable habitats for the AU and PE lineages experienced eastward range contraction. The suitable habitat area of the AU lineage decreased by 14.98%–23.22%, with habitat losses occurring primarily in northern Australian waters and the adjacent Arafura–Timor Sea. For the PE lineage, the projected habitat loss increased from 21,538.00 km² in 2051–2060 to 57,535.50 km² in 2091–2100 (Table S8, Fig. 7). Losses of suitable habitat occurred mainly along the Gulf of Oman, the Arabian Sea, and the western coast of India (Fig. 6). The WE model predicted that suitable habitat would remain relatively stable under most scenarios. However, under both the SSP5-8.5 and SSP1-2.6 scenarios, the suitable habitat contracted northward with habitat loss concentrated in the Gulf of Thailand, the central South China Sea, and waters surrounding the Philippine Islands (Table S8, Fig. 6). Overall, the species-level model showed a sustained expansion trend, whereas the lineage-level models revealed divergent habitat change patterns among lineages, particularly under SSP5-8.5 (Table S8, Figs. S20–S24).

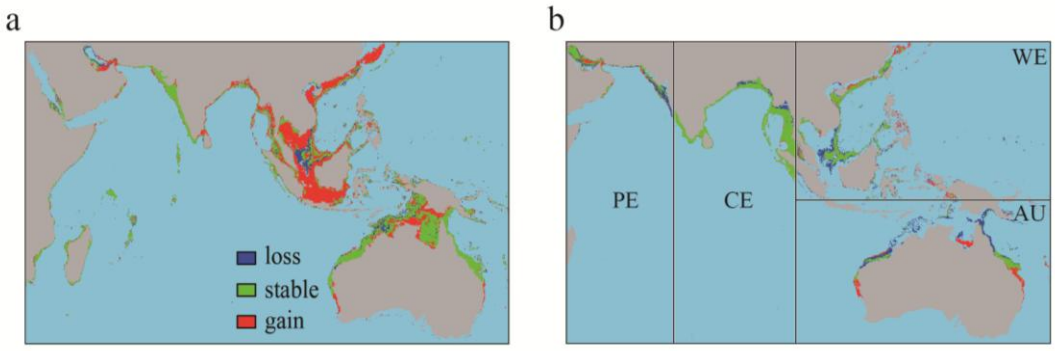


Fig. 6 Changes in the suitable habitat of *Sepia pharaonis* predicted by the species-level model (a) and lineage-level models (b) under SSP5-8.5 in 2091–2100.

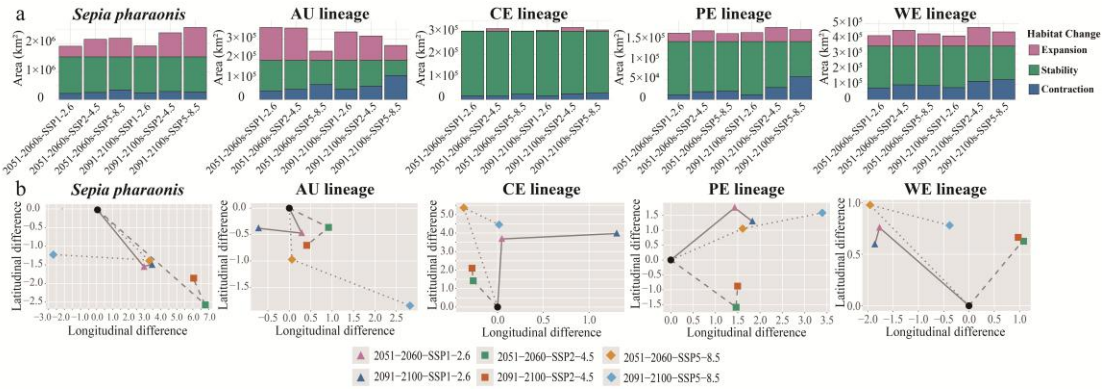


Fig. 7 Suitable habitat changes and distribution centroids of *Sepia pharaonis* at the species and lineage levels under different climate scenarios. The upper panels showed the areas of habitat contraction, stability, and expansion (a), and the lower panels showed evolution of distribution centroids of *Sepia pharaonis* (b).

Additionally, predicted shifts in suitable habitat differed markedly between the species-level and lineage-level SDMs across future climate scenarios and time periods (Fig. 7). At the species level, the centroid displacement was greater in 2091–2100 (415.37 km) than in 2051–2060 (368.63 km) under SSP1-2.6, whereas a shorter centroid displacement was projected for 2091–2100 than for 2051–2060 under SSP2-4.5 and SSP5-8.5. At the lineage level, the AU lineage showed relatively small centroid displacement under SSP1-2.6 and SSP2-4.5, but its centroid displacement increased sharply from 108.44 km in 2051–2060 to 368.43 km in 2091–2100 under SSP5-8.5. The CE lineage exhibited the greatest average centroid displacement (393.96 km) among the four lineages. The PE lineage displayed slightly reduced centroid displacement in 2091–2100 under SSP1-2.6 and SSP2-4.5, but a marked increase under SSP5-8.5, from 205.08 km in 2051–2060 to 395.66 km in 2091–2100. In contrast, the WE lineage remained almost unchanged under SSP1-2.6, decreased slightly under SSP2-4.5, and showed a substantial reduction under SSP5-8.5, from 242.17 km in 2051–2060 to 96.56 km in 2091–2100 (Table S9, Fig. 7). In addition to shifts in distribution centroids, ecological vulnerability further highlighted differences in climate change responses among lineages. The CE lineage may be more vulnerable to climate change, as its suitable habitat showed increased fragmentation under all three climate scenarios (Figs. 8 and S27). However, the WE lineage exhibited a moderate increase in vulnerability, while the AU and PE lineages remained relatively stable under most climate scenarios (Figs. S25–S29).

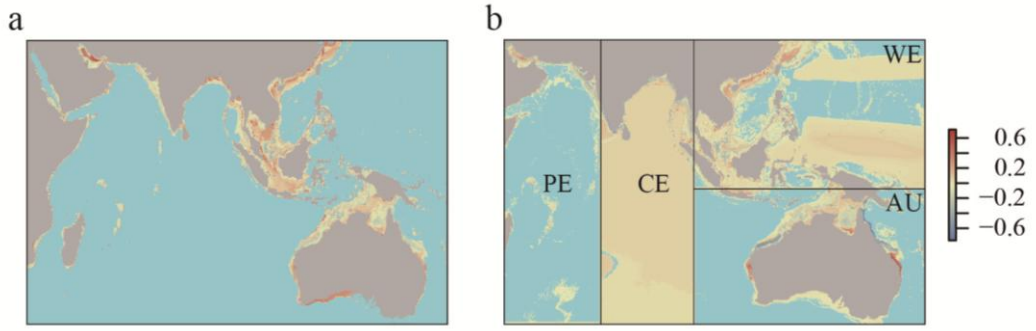


Fig. 8 Ecological vulnerability of *Sepia pharaonis* predicted by species-level model (a) and lineage-level models (b) under SSP5-8.5 in 2091–2100.

4. Discussion

4.1 Genetic diversity and differentiation of *Sepia pharaonis*

Genetic diversity analysis based on *COI* sequences revealed that the RE lineage exhibited the highest genetic diversity, whereas the WE lineage showed the lowest. The relatively high genetic diversity of the RE lineage may indicate long-term persistence of genetic variation in the Red Sea, a region recognized as an important center of phylogeographic differentiation in many marine taxa (DiBattista et al. 2016). In contrast, the particularly low genetic diversity of the WE lineage may be associated with geographic isolation and restricted gene flow (Farhadi and Anderson 2021; Li et al. 2026). These differences suggest distinct demographic histories across the five lineages, which may explain their varying responses to climate change.

The marked genetic divergence observed in *COI* and *16S* rRNA gene data, combined with the clear geographical segregation of haplotypes, may indicate cryptic species divergence in *S. pharaonis*. Limited geographical overlap among lineages and strong genetic differentiation are consistent with genetic patterns associated with incipient speciation. This highlights the importance of considering intraspecific genetic variation in projecting the potential distribution of this species when local adaptation exists.

4.2 Niche differentiation among lineages

Ecological niche analyses closely mirrored the genetic patterns, revealing substantial niche differentiation among the four lineages. The PE lineage occupied the broadest environmental niche and exhibited high genetic diversity based on analyses of *COI* sequences, suggesting that higher genetic diversity may contribute to a broader ecological niche and enhance adaptability to changing environmental conditions. This interpretation is consistent with previous studies showing positive associations between genetic variation, environmental tolerance, and niche

breadth (Sheth and Angert 2014). In contrast, the AU lineage occupied an extremely narrow niche and showed comparatively lower genetic diversity, suggesting potentially limited environmental tolerance. The high niche overlap between the CE and WE lineages suggested that they had similar environmental tolerances (Hiller et al. 2019), whereas the very limited overlap between the AU lineage and the other lineages indicated that the AU lineage may have unique environmental preferences (Cruz et al. 2023).

4.3 Intraspecific variation in SDMs

The genetic structure identified in this study provided an important basis for constructing lineage-level SDMs, because genetically differentiated populations might occupy non-equivalent climatic niches and yield substantially different projections when modeled separately (Lecocq et al. 2019; Hu et al. 2021; Zhang et al. 2021; Wu et al. 2024). Traditional SDMs generally assume niche equivalence among populations and overlook local adaptation and other forms of intraspecific variation (Pearman et al. 2010; Hällfors et al. 2016; Waldvogel et al. 2020). However, this assumption may be inappropriate for species with strong intraspecific genetic differentiation (Ikeda et al. 2017; Hu et al. 2021; Wu et al. 2024; Liu et al. 2025; Shan et al. 2025). An increasing number of studies have indicated that incorporating intraspecific variation and local adaptation into SDMs can improve the accuracy of model predictions (Collart et al. 2021; Zhang et al. 2021; Sun et al. 2022). This study demonstrated clear genetic differentiation among the five lineages and substantial niche differentiation among the four lineages of *S. pharaonis*.

Incorporating intraspecific genetic variation into distribution models could improve the ecological realism and spatial precision of model predictions (Ferrer Obiol et al. 2025). The species-level model showed broad and relatively continuous suitable habitats across northern Australian waters and the adjacent Arafura–Timor Sea under current environmental conditions. In contrast, the AU lineage-level model predicted a more restricted coastal distribution, with suitable habitats concentrated along the western and eastern coasts of Australia. A review of published literature on the distribution of *S. pharaonis* revealed that the documented distribution of the AU lineage did not extend northward into the waters of northern Australia, possibly due to temperature constraints (Ilahude et al. 2004; Jereb and Roper 2005; Anderson et al. 2007, 2011). This finding suggested that lineage-level predictions were more consistent with documented field distributions. Thus, these results indicated that constructing lineage-level SDMs might improve prediction accuracy when there is clear evidence of intraspecific genetic or niche differentiation (Zhang et al. 2021).

Habitat gain and loss analyses indicated that the species-level model yielded more optimistic projections than the lineage-level models under future climate scenarios. This situation was particularly apparent for the CE and WE lineages, as the lineage-level models predicted a contracting trend in their suitable habitat ranges under most climate scenarios, while

the species-level model predicted an obvious expanding trend. For the AU and PE lineages, the species-level model projected an expansion of the habitat range, while the lineage-level models projected habitat contraction under SSP5-8.5 (Figs. 6 and S20–S24). The divergent responses of different lineages to climate change further indicated that climate change vulnerability may vary substantially within the species, and that an overall expansion predicted at the species level does not necessarily imply that all lineages will benefit from future climate conditions. This may be because the species-level model assumed each lineage could endure all the climatic conditions that the species as a whole could tolerate (Lin et al. 2024).

4.4 Conservation and fisheries management implications

For the conservation of *S. pharaonis*, it is important to generate predictions based on precise management units defined by genetic lineages, rather than merely at the species level. The results of this study suggested that the AU and PE lineages might have stronger adaptability to climate change because they experienced habitat expansion under the SSP1-2.6 and SSP2-4.5 scenarios, whereas the CE and WE lineages were projected to experience habitat contraction under most climate scenarios. Considering the vulnerability of the CE and WE lineages to climate change, conserving these two lineages should be given a higher priority. In addition, *S. pharaonis* relies on shallow coastal waters during spawning and early life stages and is particularly vulnerable to coastal trawling and overexploitation. These anthropogenic pressures may compound the climate-driven habitat contraction and range shifts projected in this study, thereby increasing risks to populations (Hashemi and Doustdar 2021; Setyohadi et al. 2024). In conclusion, we recommend continuous monitoring of different genetic lineages and the implementation of conservation and management measures tailored to each lineage, complemented by fishing quota limits, seasonal closures during the spawning season, and marine protected areas to support the long-term sustainability of *S. pharaonis*.

5. Conclusion

This study investigated the population genetic structure of *S. pharaonis*, and the results revealed pronounced genetic differentiation among geographically distinct populations, which supported the identification of five distinct lineages. In addition, we quantified the niche differentiation among the four lineages of *S. pharaonis* and detected substantial niche divergence. Based on these findings, we developed not only species-level SDMs but also lineage-level SDMs to capture fine-scale ecological and evolutionary dynamics. We explored the response of *S. pharaonis* to climate change, taking into account intraspecific genetic variation. The different responses of the four *S. pharaonis* lineages to environmental variables indicated that lineage-level SDMs may provide more accurate predictions than species-level SDMs. The suitable habitats for the AU and PE lineages showed an overall eastward range contraction only under SSP5-8.5, suggesting low vulnerability to climate change. However, the

suitable habitats for the WE and CE lineages showed different degrees of northward range contraction under future climate scenarios, with the CE lineage exhibiting a more consistent contraction trend. These divergent trajectories demonstrated that species-level projections may mask climate-sensitive lineages and consequently lead to overly generalized management conclusions. Climate-adaptive management should therefore differentiate among lineages, prioritize monitoring and habitat conservation for the CE and WE lineages, and strengthen long-term assessment of the AU and PE lineages.

CRediT authorship contribution statement

Haomiao Chi: Writing – original draft, Investigation, Visualization, Software, Methodology, Formal analysis, Data curation, Conceptualization. Xiaoyang Wang: Writing – review & editing, Validation, Supervision, Formal analysis, Data curation, Conceptualization. Jian Zheng: Writing – review & editing, Resources, Funding acquisition. Xiaodong Zheng: Writing – review & editing, Supervision, Methodology, Conceptualization, Funding acquisition.

Declaration of generative AI use

No AI was used for this paper.

Declaration of competing interests

The authors declare no conflicts of interest.

Data availability

Data will be made available on request.

Acknowledgments

This work was supported by the Hainan Provincial Key Research and Development Program (ZDYF2026GXJS036) and the Fundamental Research Funds for the Central Universities (Grant No. 842613030).

Appendix A. Supplementary data

Supplementary data to this article can be found online at

References

Anderson FE, Valinassab T, Ho C-W, Mohamed KS, Asokan PK, Rao GS, Nootmorn P, Chotiyaputta C, Dunning M, Lu C-C (2007) Phylogeography of the pharaoh cuttle *Sepia pharaonis* based on partial mitochondrial 16S sequence data. Rev Fish Biol Fisheries 17:345-352. https://doi.org/10.1007/s11160-007-9042-1

Anderson FE, Engelke R, Jarrett K, Valinassab T, Mohamed KS, Asokan PK, Zacharia PU, Nootmorn P, Chotiyaputta C, Dunning M (2011) Phylogeny of the *Sepia pharaonis* species complex (Cephalopoda: Sepiida) based on analyses of mitochondrial and nuclear DNA sequence data. J Molluscan Stud 77(1):65-75. https://doi.org/10.1093/mollus/eyq034

Arkhipkin AI, Hendrickson LC, Payá I, Pierce GJ, Roa-Ureta RH, Robin J-P, Winter A (2021) Stock assessment and management of cephalopods: advances and challenges for short-lived fishery resources. ICES J Mar Sci 78(2):714-730. https://doi.org/10.1093/icesjms/fsaa038

Assis J, Fernández Bejarano SJ, Salazar VW, Schepers L, Gouvêa L, Fragkopoulou E, Leclercq F, Vanhoorne B, Tyberghein L, Serrão EA, Verbruggen H, De Clerck O (2024) Bio-ORACLE v3.0. Pushing marine data layers to the CMIP6 Earth System Models of climate change research. Glob Ecol Biogeogr 33(4):e13813. https://doi.org/10.1111/geb.13813

Barbet-Massin M, Jiguet F, Albert CH, Thuiller W (2012) Selecting pseudo-absences for species distribution models: how, where and how many? Methods Ecol Evol 3(2):327-338. https://doi.org/10.1111/j.2041-210X.2011.00172.x

Barratt, I., Allcock, L., 2012. *Sepia pharaonis*. *The IUCN Red List of Threatened Species* 2012, e.T162504A904257.

Blonder B, Morrow CB, Brown S, Butruille G, Chen D, Laini A, Harris DJ, Violet C (2025) hypervolume: High Dimensional Geometry, Set Operations, Projection, and Inference. R package version 3.1.6. https://doi.org/10.32614/CRAN.package.hypervolume

Breiner FT, Guisan A, Bergamini A, Nobis MP (2015) Overcoming limitations of modelling rare species by using ensembles of small models. Methods Ecol Evol 6(10):1210-1218. https://doi.org/10.1111/2041-210X.12403

Burgess MG, Becker SL, Langendorf RE, Fredston A, Brooks CM (2023) Climate change scenarios in fisheries and aquatic conservation research. ICES J Mar Sci 80(5):1163-1178. https://doi.org/10.1093/icesjms/fsad045

Cardoso P, Mammola S, Rigal F, Hilario R, Carvalho J (2026) BAT: Biodiversity Assessment Tools. R package version 2.11.1. https://doi.org/10.32614/CRAN.package.BAT

Carvalho JC, Cardoso P (2020) Decomposing the causes for niche differentiation between species using hypervolumes. Front Ecol Evol 8:243. https://doi.org/10.3389/fevo.2020.00243

Castresana J (2000) Selection of conserved blocks from multiple alignments for their use in phylogenetic analysis. Mol Biol Evol 17(4):540-552. https://doi.org/10.1093/oxfordjournals.molbev.a026334

Chardon NI, Pironon S, Peterson ML, Doak DF (2020) Incorporating intraspecific variation into species distribution models improves distribution predictions, but cannot predict

557 species traits for a wide-spread plant species. Ecography 43(1):60-74.
558 https://doi.org/10.1111/ecog.04630
559 Collart F, Hedenäs L, Broennimann O, Guisan A, Vanderpoorten A (2021) Intraspecific
560 differentiation: Implications for niche and distribution modelling. J Biogeogr 48(2):415-
561 426. https://doi.org/10.1111/jbi.14009
562 Cruz DD, Ospina-Garcés SM, Arellano E, Ibarra-Cerdeña CN, Nava-García E, Alcalá R (2023)
563 Geometric morphometrics and ecological niche modelling for delimitation of *Triatoma*
564 *pallidipennis* (Hemiptera: Reduviidae: Triatominae) haplogroups. Curr Res Parasitol
565 Vector Borne Dis 3:100119. https://doi.org/10.1016/j.crpvbd.2023.100119
566 D'Amen M, Zimmermann NE, Pearman PB (2013) Conservation of phylogeographic lineages
567 under climate change. Glob Ecol Biogeogr 22(1):93-104. https://doi.org/10.1111/j.1466-
568 8238.2012.00774.x
569 Davies SC, Thompson PL, Gomez C, Nephin J, Knudby A, Park AE, Friesen SK, Pollock LJ,
570 Rubidge EM, Anderson SC, Iacarella JC, Lyons DA, MacDonald A, McMillan A, Ward
571 EJ, Holdsworth AM, Swart N, Price J, Hunter KL (2023) Addressing uncertainty when
572 projecting marine species' distributions under climate change. Ecography
573 2023(11):e06731. https://doi.org/10.1111/ecog.06731
574 DiBattista JD, Choat JH, Gaither MR, Hobbs JPA, Lozano-Cortés DF, Myers RF, Paulay G,
575 Rocha LA, Toonen RJ, Westneat MW, Berumen ML (2016) On the origin of endemic
576 species in the Red Sea. J Biogeogr 43(1):13-30. https://doi.org/10.1111/jbi.12631
577 Di Cola V, Broennimann O, Petitpierre B, Breiner FT, D'Amen M, Randin C, Engler R, Pottier
578 J, Pio D, Dubuis A, Pellissier L, Mateo RG, Hordijk W, Salamin N, Guisan A (2017)
579 ecospat: an R package to support spatial analyses and modeling of species niches and
580 distributions. Ecography 40(6):774-787. https://doi.org/10.1111/ecog.02671
581 Elith J, Leathwick JR (2009) Species distribution models: ecological explanation and prediction
582 across space and time. Annu Rev Ecol Evol Syst 40:677-697.
583 https://doi.org/10.1146/annurev.ecolsys.110308.120159
584 Excoffier L, Lischer HEL (2010) Arlequin suite ver 3.5: a new series of programs to perform
585 population genetics analyses under Linux and Windows. Mol Ecol Resour 10(3):564-567.
586 https://doi.org/10.1111/j.1755-0998.2010.02847.x
587 Farhadi A, Anderson FE (2021) The dynasty of the pharaoh: phylogeography and cryptic
588 biodiversity of *Sepia pharaonis* cuttlefish in Northwest Indian Ocean peripheral seas. In:
589 Jawad LA (ed) The Arabian Seas: Biodiversity, Environmental Challenges and
590 Conservation Measures. Springer International Publishing, Cham, pp 427-442.
591 https://doi.org/10.1007/978-3-030-51506-5_17
592 Fernandes Guerreiro M, Oliveira Borges F, Pereira Santos C, Rosa R (2023) Future distribution
593 patterns of nine cuttlefish species under climate change. Mar Biol 170(12):159.
594 https://doi.org/10.1007/s00227-023-04310-4
595 Fernandes Guerreiro M, Oliveira Borges F, Pereira Santos C, Xavier JC, Hoving H-J, Rosa R
596 (2023) Impact of climate change on the distribution and habitat suitability of the world's
597 main commercial squids. Mar Biol 170:129. https://doi.org/10.1007/s00227-023-04261-w
598 Ferrer Obiol J, Bounas A, Brambilla M, Lombardo G, Secomandi S, Paris JR, Iannucci A,

Morganti M, Pârâu LG, Rodríguez A, Sarà M, Toli E-A, Tsiopelas N, Ciofi C, Gianfranceschi L, Jarvis ED, Olivieri A, Sotiropoulos K, Wink M, Trucchi E, Torroni A, Rubolini D (2025) Evolutionarily distinct lineages of a migratory bird of prey show divergent responses to climate change. Nat Commun 16:3503. https://doi.org/10.1038/s41467-025-58617-5

Fox-Kemper B, Hewitt HT, Xiao C, et al (2021) Ocean, cryosphere and sea level change. In: Masson-Delmotte V, Zhai P, Pirani A, et al (eds) Climate Change 2021: The Physical Science Basis. Cambridge University Press, Cambridge, UK, pp 1211-1362. https://doi.org/10.1017/9781009157896.011

Gonzalez SC, Soto-Centeno JA, Reed DL (2011) Population distribution models: species distributions are better modeled using biologically relevant data partitions. BMC Ecol 11:20. https://doi.org/10.1186/1472-6785-11-20

Hällfors MH, Liao J, Dzurisin J, Grundel R, Hyvärinen M, Towle K, Wu GC, Hellmann JJ (2016) Addressing potential local adaptation in species distribution models: implications for conservation under climate change. Ecol Appl 26:1154-1169. https://doi.org/10.1890/15-0926

Hashemi SA, Doustdar M (2021) Optimized exploitation of Pharaoh cuttlefish (*Sepia pharaonis* Ehrenberg, 1831) stocks in the Iranian part of Persian Gulf and Oman Sea. Int J Aquat Biol 9(2):97-104. https://doi.org/10.22034/ijab.v9i2.736

Hiller AE, Koo MS, Goodman KR, Shaw KL, O'Grady PM, Gillespie RG (2019) Niche conservatism predominates in adaptive radiation: comparing the diversification of Hawaiian arthropods using ecological niche modelling. Biol J Linn Soc 127:479-492. https://doi.org/10.1093/biolinnean/blz023

Hu ZM, Zhang QS, Zhang J, Kass JM, Mammola S, Fresia P, Draisma SGA, Assis J, Jueterbock A, Yokota M, Zhang Z (2021) Intraspecific genetic variation matters when predicting seagrass distribution under climate change. Mol Ecol 30:3840-3855. https://doi.org/10.1111/mec.15996

Huang H, Zhou Z, Peng D, Chu J (2024) Potential impacts of climate change on cephalopods in a highly productive region (Northwest Pacific): habitat suitability and management. Sci Total Environ 953:175794. https://doi.org/10.1016/j.scitotenv.2024.175794

Ikeda DH, Max TL, Allan GJ, Lau MK, Shuster SM, Whitham TG (2017) Genetically informed ecological niche models improve climate change predictions. Glob Chang Biol 23:164-176. https://doi.org/10.1111/gcb.13470

Ilahude AG, Hortle K, Kusmanto E, Amiruddin (2004) Oceanography of coastal and riverine waters around Timika, West Central Irian Jaya, Arafura Sea. Cont Shelf Res 24:2511-2520. https://doi.org/10.1016/j.csr.2004.07.020

Jereb, P., Roper, C.F.E. (Eds.), 2005. *Cephalopods of the world: An annotated and illustrated catalogue of cephalopod species known to date. Volume 1. Chambered nautiluses and sepioids (Nautilidae, Sepiidae, Sepiolidae, Sepiadariidae, Idiosepiidae and Spirulidae).* FAO Species Catalogue for Fishery Purposes, No. 4, Vol. 1. FAO, Rome, 262 pp.

Johnston R, Jones K, Manley D (2018) Confounding and collinearity in regression analysis: a cautionary tale and an alternative procedure, illustrated by studies of British voting

behaviour. Qual Quant 52:1957-1976. https://doi.org/10.1007/s11135-017-0584-6

Katoh K, Misawa K, Kuma K, Miyata T (2002) MAFFT: a novel method for rapid multiple sequence alignment based on fast Fourier transform. Nucleic Acids Res 30:3059-3066. https://doi.org/10.1093/nar/gkf436

Kumar S, Stecher G, Suleski M, Sanderford M, Sharma S, Tamura K (2024) MEGA12: Molecular evolutionary genetic analysis version 12 for adaptive and green computing. Mol Biol Evol 41:msae263. https://doi.org/10.1093/molbev/msae263

Lecocq T, Harpke A, Rasmont P, Schweiger O (2019) Integrating intraspecific differentiation in species distribution models: consequences on projections of current and future climatically suitable areas of species. Divers Distrib 25:1088-1100. https://doi.org/10.1111/ddi.12916

Leigh JW, Bryant D (2015) popart: full-feature software for haplotype network construction. Methods Ecol Evol 6:1110-1116. https://doi.org/10.1111/2041-210X.12410

Letunic I, Bork P (2024) Interactive Tree of Life (iTOL) v6: recent updates to the phylogenetic tree display and annotation tool. Nucleic Acids Res 52:W78-W82. https://doi.org/10.1093/nar/gkae268

Li L, Zhao L, Fu J, Sun B, Liu C (2022) Predicting the habitat suitability for populations of Pacific cod under different climate change scenarios considering intraspecific genetic variation. Ecol Indic 142:109248. https://doi.org/10.1016/j.ecolind.2022.109248

Li YL, Long JK, Chang ZM, Wang HC, Meng JY, Yang L, Gao JY, Chen XS (2026) Genetic diversity of *Spodoptera litura* in China based on mitochondrial DNA analysis. Phytoparasitica 54:29. https://doi.org/10.1007/s12600-025-01348-6

Lin XN, Ma CY, Hu LS, Liao ML, Ma LX, Teske PR, Hoffmann A, Dong YW (2024) Genomics-informed range predictions under global warming reveal reduced adaptive diversity whilst buffering range shifts for a marine snail. Glob Chang Biol 30:e17571. https://doi.org/10.1111/gcb.17571

Liu K, Tao Y, Huang W, Wang B, Liu S, Cong B, Zhou M, Zhao L (2025) Assessment of future habitat suitability and ecological vulnerability of *Collichthys* at population and species level. BMC Ecol Evol 25:1. https://doi.org/10.1186/s12862-024-02339-7

Lu WX, Wang ZZ, Hu XY, Rao GY (2024) Incorporating eco-evolutionary information into species distribution models provides comprehensive predictions of species range shifts under climate change. Sci Total Environ 912:169501. https://doi.org/10.1016/j.scitotenv.2023.169501

Mahmud HB, Osawa T (2026) Assessment of coastal erosion along the Kelantan shoreline in response to projected sea level rise under various shared socioeconomic pathways (SSP). IOP Conf Ser Earth Environ Sci 1599:012028. https://doi.org/10.1088/1755-1315/1599/1/012028

Mammola S, Cardoso P (2020) Functional diversity metrics using kernel density n-dimensional hypervolumes. Methods Ecol Evol 11:986-995. https://doi.org/10.1111/2041-210X.13424

Manzoor SA, Griffiths G, Lukac M (2018) Species distribution model transferability and model grain size–finer may not always be better. Sci Rep 8:7168. https://doi.org/10.1038/s41598-018-25437-1

683 Marmion M, Parviainen M, Luoto M, Heikkinen RK, Thuiller W (2009) Evaluation of
684 consensus methods in predictive species distribution modelling. Divers Distrib 15:59-69.
685 https://doi.org/10.1111/j.1472-4642.2008.00491.x

686 McMahan CD, Fuentes-Montejo CE, Ginger L, Carrasco JC, Chakrabarty P, Matamoros WA
687 (2020) Climate change models predict decreases in the range of a microendemic
688 freshwater fish in Honduras. Sci Rep 10:12693. https://doi.org/10.1038/s41598-020-
689 69579-7

690 Ottmann D, Andersen KH, van Denderen PD (2024) Biomass and trait biogeography of
691 cephalopods on the European and North American continental shelves. Glob Ecol
692 Biogeogr 33:439-449. https://doi.org/10.1111/geb.13803

693 Palmegiano GB, D'Apote MP (1983) Combined effects of temperature and salinity on cuttlefish
694 (*Sepia officinalis* L.) hatching. Aquaculture 35:259-264. https://doi.org/10.1016/0044-
695 8486(83)90096-0

696 Pearman PB, D'Amen M, Graham CH, Thuiller W, Zimmermann NE (2010) Within-taxon niche
697 structure: niche conservatism, divergence and predicted effects of climate change.
698 Ecography 33:990-1003. https://doi.org/10.1111/j.1600-0587.2010.06443.x

699 Pecl GT, Jackson GD (2008) The potential impacts of climate change on inshore squid: biology,
700 ecology and fisheries. Rev Fish Biol Fish 18:373-385. https://doi.org/10.1007/s11160-
701 007-9077-3

702 Peng RB, Wang PS, Jiang MW, Ruan P, Han QX, Jiang XM (2017) Effect of salinity on
703 embryonic development of the cuttlefish *Sepia pharaonis*. J World Aquac Soc 48:666-675.
704 https://doi.org/10.1111/jwas.12321

705 Rozas J, Ferrer-Mata A, Sánchez-DelBarrio JC, Guirao-Rico S, Librado P, Ramos-Onsins SE,
706 Sánchez-Gracia A (2017) DnaSP 6: DNA sequence polymorphism analysis of large data
707 sets. Mol Biol Evol 34:3299-3302. https://doi.org/10.1093/molbev/msx248

708 Sampaio E, Santos C, Rosa IC, Ferreira V, Pörtner HO, Duarte CM, Levin LA, Rosa R (2021)
709 Impacts of hypoxic events surpass those of future ocean warming and acidification. Nat
710 Ecol Evol 5:311-321. https://doi.org/10.1038/s41559-020-01370-3

711 Sasikumar G, Mohamed KS, Bhat US (2013) Inter-cohort growth patterns of pharaoh cuttlefish
712 *Sepia pharaonis* (Sepioidea: Sepiidae) in Eastern Arabian Sea. Rev Biol Trop 61:1-14.
713 https://doi.org/10.15517/rbt.v61i1.10871

714 Schickele A, Francour P, Raybaud V (2021) European cephalopods distribution under climate-
715 change scenarios. Sci Rep 11:3930. https://doi.org/10.1038/s41598-021-83457-w

716 Setyohadi D, Rahman MA, Harlyan LI, Rihmi MK (2024) Species identification and population
717 dynamics of cuttlefish *Sepia* spp. (Mollusca: Cephalopoda) landed at Brondong Fishing
718 Port, Lamongan, East Java, Indonesia. Biodiversitas 25:1359-1367.
719 https://doi.org/10.13057/biodiv/d250403

720 Shan B, Huang W, Zhang M, Wang L, Liu Y, Yan C, Liu M, Xie Q, Zou J, Zhao L, Sun D (2025)
721 Integrating population genetics and species distribution models to predict red seabream
722 distribution under climate change. Glob Ecol Conserv 60:e03589.
723 https://doi.org/10.1016/j.gecco.2025.e03589

724 Sheth SN, Angert AL (2014) The evolution of environmental tolerance and range size: a

725 comparison of geographically restricted and widespread Mimulus. Evolution 68:2917-
726 2931. https://doi.org/10.1111/evo.12494

727 Sillero N, Arenas-Castro S, Enriquez-Urzelai U, Vale CG, Sousa-Guedes D, Martínez-Freiría
728 F, Real R, Barbosa AM (2021) Want to model a species niche? A step-by-step guideline
729 on correlative ecological niche modelling. Ecol Model 456:109671.
730 https://doi.org/10.1016/j.ecolmodel.2021.109671

731 Song W, Li R, Zhao Y, Migaud H, Wang C, Bekaert M (2021) Pharaoh cuttlefish, *Sepia*
732 *pharaonis*, genome reveals unique reflectin camouflage gene set. Front Mar Sci 8:639670.
733 https://doi.org/10.3389/fmars.2021.639670

734 Sun B, Zhao L, Shao F, Lu Z, Tian J, Liu C (2022) Estimating the impacts of climate change
735 on the habitat suitability of common minke whales integrating local adaptation. Front Mar
736 Sci 9:923205. https://doi.org/10.3389/fmars.2022.923205

737 Thuiller W, Georges D, Gueguen M, Engler R, Breiner F, Lafourcade B, Patin R, Blancheteau
738 H (2024) *biomod2: Ensemble platform for species distribution modeling*. R package
739 version 4.2-6-2. https://biomodhub.github.io/biomod2/

740 Turan C, Soldo A (2026) Projected habitat contraction and distributional shifts of the near
741 threatened undulate ray *Raja undulata* under climate change. Biology 15:1035.
742 https://doi.org/10.3390/biology15131035

743 Tyberghein L, Verbruggen H, Pauly K, Troupin C, Mineur F, De Clerck O (2012) Bio-ORACLE:
744 a global environmental dataset for marine species distribution modelling. Glob Ecol
745 Biogeogr 21:272-281. https://doi.org/10.1111/j.1466-8238.2011.00656.x

746 Vinagre C, Almeida L, Ronquillo P, Mendonça V, Frade D, Gonçalves EJ, Erzini K, Serrão EA
747 (2025) Network analysis reveals humans as top predators and the key role of cuttlefish in
748 the food web structure of a marine protected area (Arrábida Natural Park). Ecol Complex
749 63:101134. https://doi.org/10.1016/j.ecocom.2025.101134

750 Waldvogel AM, Feldmeyer B, Rolshausen G, Exposito-Alonso M, Rellstab C, Kofler R, Mock
751 T, Schmid K, Schmitt I, Bataillon T, Savolainen O, Bergland A, Flatt T, Guillaume F,
752 Pfenninger M (2020) Evolutionary genomics can improve prediction of species' responses
753 to climate change. Evol Lett 4:4-18. https://doi.org/10.1002/evl3.154

754 Wang X, Zheng J, Li J, Xiao S, Zheng X (2026) Potential impacts of climate change and fishing
755 pressure on important cephalopods in Northwest Pacific: applications for conservation and
756 management of vulnerable habitats. J Environ Manage 397:128242.
757 https://doi.org/10.1016/j.jenvman.2025.128242

758 Wu K, Xin H, Yuan Y, Zhao Y, Song W, Wang C, Mu C, Li R (2021) Physiological, biochemical
759 and molecular responses of *Sepia pharaonis* juveniles to low salinity. Aquac Res 52:4317-
760 4324. https://doi.org/10.1111/are.15269

761 Wu Z, Dong H, Li L, Zhao L, Song N (2024) Lineage-level species distribution model to assess
762 the impact of climate change on the habitat suitability of *Boleophthalmus pectinirostris*.
763 Front Ecol Evol 12:1364822. https://doi.org/10.3389/fevo.2024.1364822

764 Xiang S, Jin P, Cao J, Yu W (2025) Environmental effects on cephalopod community structure
765 and distribution on the eastern Bering Sea upper continental slope. Mar Environ Res
766 210:107353. https://doi.org/10.1016/j.marenvres.2025.107353

767 Zhang Z, Kass JM, Mammola S, Koizumi I, Li X, Tanaka K, Ikeda K, Suzuki T, Yokota M,
768 Usio N (2021) Lineage-level distribution models lead to more realistic climate change
769 predictions for a threatened crayfish. Divers Distrib 27:684-695.
770 https://doi.org/10.1111/ddi.13225
771 Zheng J, Li Q, Zheng X (2023) Ocean acidification increases copper accumulation and
772 exacerbates copper toxicity in *Amphioctopus fangsiao* (Mollusca: Cephalopoda): a
773 potential threat to seafood safety. Sci Total Environ 891:164473.
774 https://doi.org/10.1016/j.scitotenv.2023.164473
775 Zheng J, Li S, Zheng X (2024) Living in a dynamic environment: the effects of multi-ways
776 temperature variation on embryo and newborn juveniles of a shallow-water octopus
777 (*Amphioctopus fangsiao*). Sci Total Environ 923:171510.
778 https://doi.org/10.1016/j.scitotenv.2024.171510
779 Zurell D, Franklin J, König C, Bouchet PJ, Dormann CF, Elith J, Fandos G, Feng X, Guillera-
780 Arroita G, Guisan A, Lahoz-Monfort JJ, Leitão PJ, Park DS, Peterson AT, Rapacciuolo G,
781 Schmatz DR, Schröder B, Serra-Diaz JM, Thuiller W, Yates KL, Zimmermann NE, Merow
782 C (2020) A standard protocol for reporting species distribution models. Ecography
783 43:1261-1277. https://doi.org/10.1111/ecog.04960

Supplementary Files

This is a list of supplementary files associated with this preprint. Click to download.

- SupplementaryMaterial.docx